Chiroptical Properties of the Cisoid Enone Chromophore

Jadwiga Frelek,*,† Wojciech J. Szczepek,‡ Hans Peter Weiss,§ Guido J. Reiss,⊥ Walter Frank,⊥ Joachim Brechtel,⊥ Bernd Schultheis,⊥ and Hans-Georg Kuball*,⊥

Contribution from the Institute of Organic Chemistry of the Polish Academy of Sciences, PL-01-224 Warszawa, Kasprzaka 44, Poland, Pharmaceutical Research Institute, PL-01-793 Warszawa, Rydygiera 8, Poland, Department of Chemistry, Ruhr-University Bochum, D-44780 Bochum, Universitätstrasse 150, and Department of Chemistry, University of Kaiserslautern, D-67663 Kaiserslautern, Erwin-Schrödinger-Strasse, Germany

Received September 2, 1997

Abstract: The circular dichroism (CD) and circular dichroism of anisotropic samples (ACD) of cisoid enones 3-methyl-3α,5α-3,3′,4′,5′-tetrahydrobenzo[2,3]cholest-2-en-1-one (**4**) and its 3β-diastereoisomer **7** have been investigated. The relation between structures, obtained from energy minimization and from X-ray analysis, and the signs of the Cotton effects (CEs) is discussed in terms of previously published rules.[1,2] A modification of recently published rules connecting signs of the nπ* and band II CEs with enone chirality is postulated. The ACD results allow an interpretation of the breakdown of the helicity rule for the nπ* band of **7** as a consequence of a different variation of the different coordinates $\Delta\epsilon^*_{ii}$ in $\Delta\epsilon = (\Delta\epsilon^*_{11} + \Delta\epsilon^*_{22} + \Delta\epsilon^*_{33})/3$ by vibronic coupling in comparison to the coordinates $\Delta\epsilon^*_{ii}$ of **4**. This change of the size of the $\Delta\epsilon^*_{ii}$ of **7** originates from a different perturbation of the enone chromophore by the cyclohexene A′ ring which causes a non-symmetrically deformed A ring system in **7** (non-symmetrical boat conformation) compared with the slightly distorted symmetrical chair conformation in **4**.

In a recent paper on circular dichroism (CD) of steroidal and related cisoid enones[1] we have shown that the sign of the enone torsion angle correlates with the sign of the nπ* Cotton effect (CE). In the case of a bisignate curve within the nπ* transition the enone helicity corresponds to the sign of the long wavelength part of the nπ* CE. Furthermore, the sign of the band II CE of around 200 nm is opposite to that of nπ* CE.[2] However, nardosinon **A** shows a positive nπ* Cotton effect,[3] although its conformational analysis by molecular mechanics calculations[4] indicates a negative enone torsion angle (Figure 1). Its cyclopropyl derivative **B** exhibits a bisignate CD curve in the nπ* region with a strong positive CD band followed by a small negative long wavelength part of this band. Only one negative band for nπ* transition is found for nardosinondiol **C**. This negative sign, as well as the negative sign of the long wavelength part of the nπ* band of **B**, corresponds to the enone helicity of both **B** and **C** nardosinon derivatives, thus holding to the aforementioned rule for the nπ* band.

In view of these data the question arises whether compound **A** is an exception to the rule or, in other words, the rule is imperfect. The question for the origin of this break down of the rule is of large importance. Is there an example given where although the first sphere, the enone-chromophore, is inherently dissymmetric, the second sphere, i.e., the conformation of the cyclohexanone unit, influences the sign of the nπ* CE? To solve this problem, we decided to synthesize suitable model compounds, to determine their geometries and to compare the structural parameters with the CD data. Besides that, the ACD spectroscopy (CD spectroscopy of anisotropic samples, i.e., of oriented molecules) is used in order to obtain additional information.

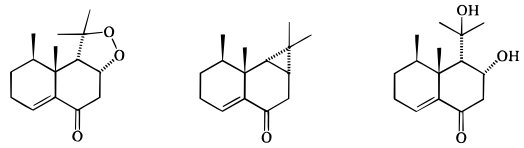

	A	**B**	**C**
nπ* CE (acetonitrile);			
$\Delta\varepsilon(\lambda)$:	+0.75 (343)	−0.01 (393) +0.29 (327)	−1.15 (336)
enone torsion angles of the two lowest energy conformers (MMX calculations):	−37° and −10°	−37° and −19°	−33° and −31°

Figure 1. Nardosinon **A**−**C** derivatives.

Synthesis of Enones 4 and 7

The simplest ways to target cisoid enones are condensation of an additional ring to a readily available steroid or another transoid enone and, if possible, transformation of the obtained cisoid enone to the next one with reversed enone moiety. Such synthetic strategy has been used in obtaining two different cisoid enones from (−)-verbenone.[2] From among cholestane derivatives only cholest-1-en-3-ones, cholest-2-en-1-ones, cholest-2-en-4-ones, or cholest-3-en-2-ones could be used for this purpose. Therefore, we decided to synthesize two isomeric cisoid enones **4** and **7** starting from the most readily available 5α-cholest-1-en-3-one (**1**, Scheme 1).

† Polish Academy of Sciences.
‡ Pharmaceutical Research Institute.
§ Ruhr-University Bochum.
⊥ University of Kaiserslautern.

(1) Frelek, J.; Szczepek, W. J.; Weiss, H. P. *Tetrahedron: Asymmetry* **1995**, *6*, 1419−1430.
(2) Frelek, J.; Szczepek, W. J.; Weiss, H. P. *Tetrahedron: Asymmetry* **1993**, *4*, 411−424.
(3) Snatzke, G.; Rücker, G. Unpublished results.
(4) PC Model 4.0.

S0002-7863(97)03076-X CCC: $15.00
Published on Web 06/29/1998

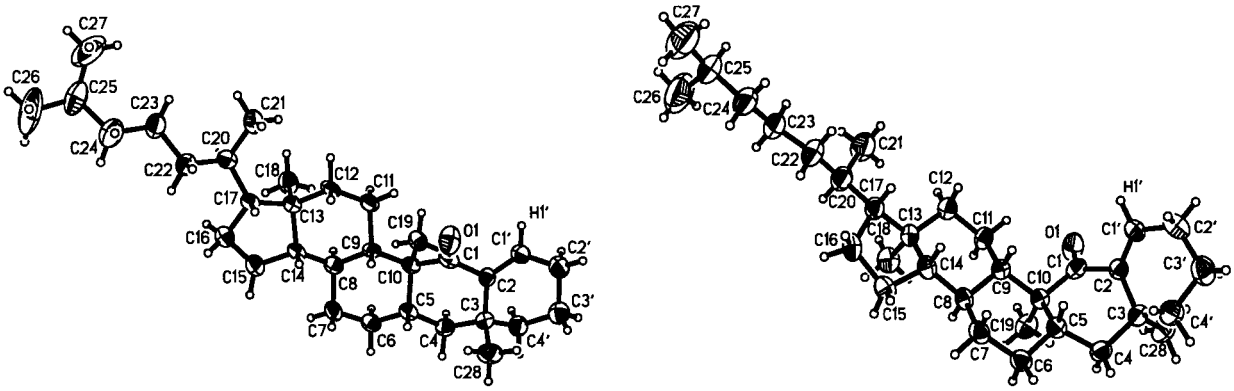

Figure 2. Diagrams[10] of **4** (left) and **7** (right) showing the atom-numbering schemes. Displacement ellipsoids are shown at the 50% probability level, and H atoms are drawn as unlabeled spheres of arbitrary size. (Numbering of atoms in the ring A′ as used in the crystallographic analysis.)

Scheme 1

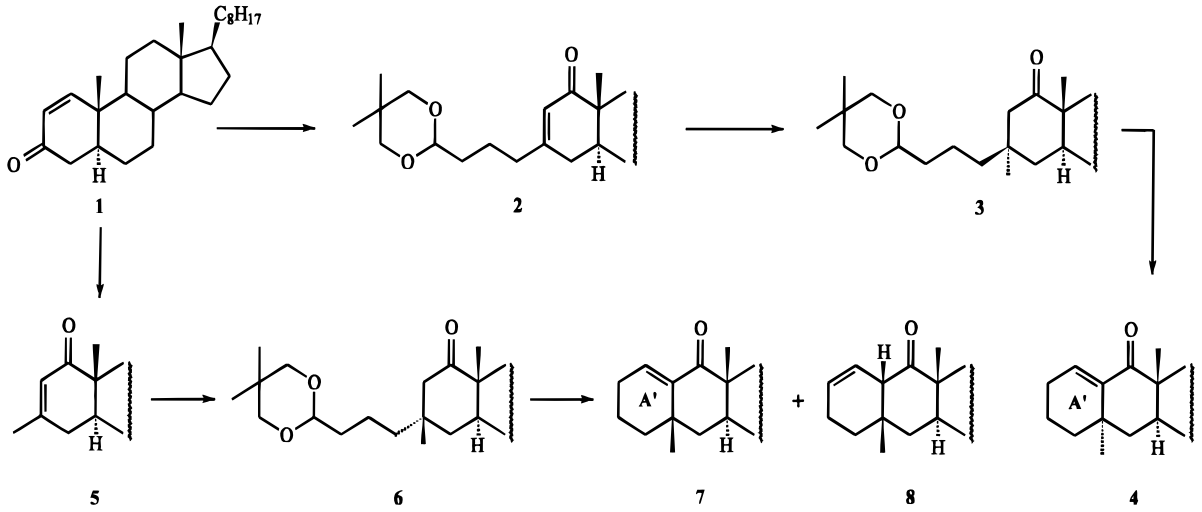

The synthesis of the two model enones **4** and **7** was achieved with the use of the same substrates namely 5α-cholest-1-en-3-one and protected 4-bromobutanal. Regioselective addition of the Grignard reagent prepared from protected 4-bromobutanal to the trans enone **1** and oxidation of the crude allylic tertiary alcohol gives *β*-substituted *trans*-enone **2**. Its regio- and stereospecific methylation leads to introduction of 3α-methyl substituent thus giving the first desired intermediate **3**. One-pot deprotection of the acetal, aldol condensation, and dehydration gives the target all-trans condensed cisoid enone **4** bearing an axial methyl substituent at the α′-position (the nomenclature of positions according to Gawronski[5]). The reverse sequence of alkylation reactions, i.e., addition of methyllithium to the substrate **1**, oxidation of the resulting allylic tertiary alcohol to the *trans*-enone **5**, and its subsequent alkylation with a reagent prepared from protected 4-bromobutanal gives the second desired intermediate **6**. Treatment of this compound with concentrated hydrochloric acid in boiling dioxane affords a mixture of the target cisoid enone **7** and its *β*,*γ*-unsaturated isomer, ketone **8**.

X-ray Structure Determinations

Crystals of **4** and **7** suitable for X-ray study were obtained by slow evaporation of the solvent from ethanol solutions. They were investigated on an Enraf-Nonius CAD4 diffractometer using graphite-monochromated Cu Kα radiation ($\lambda = 1.54184$ Å). Unit cell parameters were determined by least-squares refinement[6] on diffractometer angles for 24 and 25 automatically centered reflections in the range $15.4° < \theta < 26.6°$ and $14.0° < \theta < 20.0°$, respectively. Throughout the intensity data measurements[6] in the $\omega/2\theta$ scan mode no significant alterations were observed in the three control intensities monitored every 60 min.[7] In the case of **4**, symmetry of the diffraction pattern and systematic absences were consistent with the monoclinic space groups $P2_1$ and $P2_1/m$, but the second can be ruled out, because it is not possible for a single enantiomorph of a chiral compound. In the case of **7** the orthorhombic space group $P2_12_12$ was uniquely determined. The program SHELXS-86[8] was used for primary structure solution by direct methods, the program SHELXL-93[9] for secondary structure solution and refinement. The final full-matrix least-squares refinements on F^2 involved an anisotropic model for all atoms heavier than hydrogen (Figure 2). With the exception of H1′, whose atomic coordinates were treated without restraints for both compounds, all hydrogen atoms were included in the refinements in calculated positions and allowed to ride on the carbon atoms to

(5) Gawronski, J. K. *Tetrahedron* **1982**, *38*, 3.

(6) *CAD4 Software*; Version 5.0, Enraf-Nonius: Delft, The Netherlands, 1989.

(7) Harms, K.; Wocadlo, S. *XCAD4. Program to Extract Intensity Data from Enraf-Nonius CAD4 File*; University of Marburg: Germany, 1993.

(8) Sheldrick, G. M. *SHELXS86. Program for the Solution of Crystal Structures*; University of Göttingen: Germany, 1985.

(9) Sheldrick, G. M. *SHELXL93. Program for the Refinement of Crystal Structures*; University of Göttingen: Germany, 1992.

(10) Sheldrick, G. M. *SHELXTL-Plus*, Realease 4.22; Siemens Analytical X-ray Instruments Inc.: Madison, WI, 1991.

(11) Eliel, E. L.; Wilen, S. H.; Mander, L. N. *Stereochemistry of organic compounds*; John Wiley & Sons Ltd.: New York, 1994; p 1193.

Table 1. Selected Crystallographic Data[a]

compound	**4**	**7**
chemical formula	$C_{32}H_{52}O$	$C_{32}H_{52}O$
formula weight	452.74	452.74
space group	$P2_1$	$P2_12_12$
a, Å	11.905(2)	20.503(4)
b, Å	7.3620(10)	21.729(4)
c, Å	16.112(3)	6.3890(10)
β, deg	95.597(9)	90.0
V, Å^3	1405.4(4)	2846.4(9)
Z	2	4
T, K	293(2)	291(2)
density, g/cm^3	1.070	1.056
μ(Cu Kα), mm^{-1}	0.457	0.452
no. of reflns meas	6602	6786
no. of indep reflns	3308	4719
no. of params refined	379	380
no. of reflns used	2851 ($I > 0$)	4719
$R(F)[F^2 > 2\sigma(F^2)]$	0.053	0.063
$wR(F^2)$	0.066	0.088

[a] $R = \sum||F_o| - |F_c||/\sum|F_o|$; $wR = [\sum w(F_o^2 - F_c^2)^2/w(F_o^2)^2]^{1/2}$.

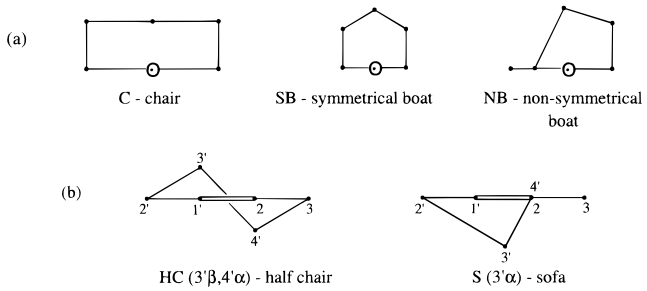

Figure 3. Idealized conformations of cyclohexanone (a) and cyclohexene (b) rings of cisoid enones. In the case of cyclohexene ring projections the enone carbonyl group lies on the right side of the double bond. The numbering of carbon atoms are as given in crystal structure of **4** and **7 (**Figure 2).

which they are attached; the isotropic displacement parameters were kept equal to 120%, 130%, and 150% of the equivalent isotropic displacement parameters of the parent tertiary, secondary, and primary carbon atom, respectively. Scattering factors, dispersion corrections, and absorption coefficients were taken from *International Tables for Crystallography* (1992, Vol. C, Tables 6.1.1.4, 4.2.6.8, and 4.2.4.2). Crystal data and final *R* values are given in Table 1. Table 2 provides some relevant bond lengths, angles, and torsion angles (See also Supporting Information).

Conformations of Enones 4 and 7

The cyclohexanone ring of the enone **4**, belonging to the class of all-trans condensed compounds, should adopt chair or slightly distorted chair conformation. In the case of the enone **7** nonsymmetrical boat (NB, Figure 3a) conformation of the cyclohexanone unit could be expected from inspection of Dreiding models and from MMX calculations. The chair or slightly distorted chair conformation of the cyclohexanone ring is characteristic for least energy conformers of all-trans condensed cisoid enones until now studied.[1] Boat or distorted boat conformations are mostly expected for remaining condensed systems, as in the case of 1β,4′,5′,6′-tetrahydrobenzo[1,2]-5α-cholest-1-en-3-one[1,2] (slightly distorted SB conformation, Figure 3a).

Conformational analysis by molecular mechanics calculations using MMX program[4] reveals that cyclohexanone ring in the two conformers of lowest energy of all-trans condensed enone **4**, which differ in energy by 1.46 kcal/mol, adopts a distorted

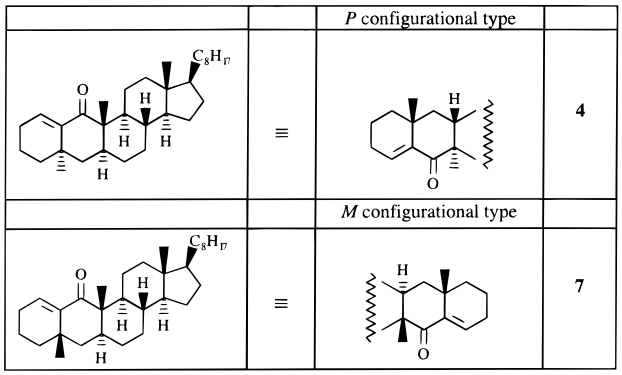

Figure 4. Structures of enones **4** and **7** and their configurational assignment with respect to the torsional angle C(1′)═C(2)─C(3)─C(28) after the work of Gawronski.[5,14] The helicity of the enone O(1)═C(1)─C(2)═C(1′) is *M* and *P*, respectively.

chair conformation. Both methyl substituents at C-3 and C-10 are quasi-axially oriented. The cyclohexene ring of the least energy conformer exists in HC (3′β,4′α) conformation, whereas that of the next lowest energy conformer is close to S (3′α) conformation (Figure 3b). The calculated enone torsion angles O(1)═C(1)─C(2)═C(1′) are ca. −56° and −66°, respectively. The calculations done for cisoid enone **7** show that cyclohexanone ring of its two lowest energy conformers differing in energy by 1.9 kcal/mol adopts distorted non-symmetrical boat conformation (NB), which idealized projections show Figure 3a. The cyclohexene ring of the least energy conformer exists in a distorted HC (3′α,4′β), whereas that of the second conformer is close to S (3′β) conformation (Figure 3b). The obtained enone torsion angles O(1)═C(1)─C(2)═C(1′) of this enone are ca. +52° and +64°, respectively. Methyl substituent at C-3 is quasi-axially oriented but the methyl group at C-10 and the C(10)─C(9) bond are neither axially nor equatorially oriented. They lie nearly symmetrically to the C(10)─C(1)─C(2) plane showing a bisecting conformation.[11,12]

Chiroptical Properties

Circular Dichroism (CD). The nπ* CD band of enone **4** (Table 3, Figure 5) is bisignate in isooctane, acetonitrile, and ethanol and becomes a monosignate CD curve in trifluoroethanol and 1%trifluoroacetic acid in isooctane. According to the helicity rule it should be negative and, consequently, the stronger long wavelength part in a bisignate band or the monosignate band is negative. The appearance of a positive part of a band in the nπ* transition at shorter wavelengths may be attributed to a positive CD of a vibronic progression intensified by the disturbance of the chromophore by the axial methyl substituent at α′-position, similarly as in the case of the 7α-bromosubstituted cholest-4-en-6-ones.[1] The low-temperature measurements (Table 4) done for nπ* CE of enone **4** still show the presence of a bisignate curve with a positive part of nearly the same intensity and a negative one of slowly increasing magnitude on going from +20 °C to −160 °C. The band I CE of enone **4** is strongly positive and follows the original orbital helicity rule.[13] The blue shift of the nπ* CE and red one of the band I CE is evidently seen on going from nonpolar to polar solvents (Table 3, Figure 5, left). Band II CE is well-separated from band I CE, and its maximum lying below 200 nm is reached only in acetonitrile and trifluoroethanol. The positive sign of this band

(12) Lightner, D. A. *The Octant Rule* in *Circular Dichroism: Principles and Applications;* Nakanishi, K., Berova, N., Woody, R. W., Eds.; VCH Publishers: New York, 1994; pp 259−299.

(13) Kirk, D. N. *Tetrahedron* **1986**, *42*, 777−818.

Table 2. Selected Geometric Parameters (Å or deg)

	4	**7**		**4**	**7**
			bond lengths		
O1−C1	1.222(4)	1.220(3)	C10−C1	1.513(5)	1.523(4)
C1−C2	1.510(5)	1.511(4)	C2−C1′	1.325(6)	1.313(4)
C2−C3	1.510(6)	1.506(4)	C1′−C2′	1.506(6)	1.493(4)
C3−C4	1.524(5)	1.555(4)	C2′−C3′	1.540(5)	1.496(4)
C4−C5	1.536(5)	1.535(3)	C3′−C4′	1.515(5)	1.520(4)
C5−C10	1.546(5)	1.536(4)	C4′−C3	1.541(5)	1.541(4)
			valence angles		
O1−C1−C2	120.6(4)	120.9(3)	C5−C10−C1	105.5(3)	108.4(2)
O1−C1−C10	123.7(4)	122.6(3)	C2−C3−C4′	109.8(4)	107.8(3)
C2−C1−C10	115.7(4)	116.5(3)	C2−C1′−C2′	124.5(5)	123.6(3)
C1−C2−C3	117.5(4)	115.8(3)	C1′−C2′−C3′	112.3(4)	112.4(3)
C2−C3−C4	111.5(4)	110.8(2)	C1′−C2−C3	123.4(4)	125.4(3)
C3−C4−C5	113.9(4)	111.5(2)	C2′−C3′−C4′	111.0(4)	111.1(3)
C4−C5−C10	112.5(4)	111.4(2)	C3′−C4′−C3	112.4(4)	112.5(3)
			torsion angles		
O1−C1−C2−C1′	−45.9(6)	56.5(4)	C2′−C1′−C2−C3	3.6(7)	−2.4(5)
C1−C2−C3−C4	38.4(5)	−37.1(4)	C2−C1′−C2′−C3′	−13.0(7)	13.8(4)
C2−C3−C4−C5	−43.3(5)	−17.5(4)	C1′−C2′−C3′−C4′	39.9(5)	−41.8(4)
C3−C4−C5−C10	57.1(5)	64.4(3)	C2′−C3′−C4′−C3	−59.7(5)	61.2(4)
C4−C5−C10−C1	−59.3(4)	−51.2(3)	C2−C3−C4′−C3′	48.5(5)	−47.0(4)
C5−C10−C1−C2	54.2(5)	−3.9(3)	C19−C10−C1−O1	114.4(4)	50.8(4)
C10−C1−C2−C3	−46.8(5)	50.6(3)	C9−C10−C1−O1	−7.5(6)	−69.1(4)
C1′−C2−C3−C4′	−20.8(6)	18.8(4)	C1′−C2−C3−C28	98.8(5)	−101.2(4)

Table 3. UV and CD Data of **4** and **7** in Different Solvents

		ϵ (λ_{max}/nm)		$\Delta\epsilon$ (λ_{max}/nm)			
				nπ*			
compd	solvent[a]	nπ*	$\pi\pi$*			band I	band II
4	Oct	54 (323)	6500 (228)	−0.65 (331)	+0.27 (288)	+9.18 (227)	+[b]
	Ace	84 (317)	5700 (232)	−0.76 (326)	+0.16 (286)	+8.07 (231)	+14.6 (188)
	Eth	110 (310)	5600 (234)	−0.91 (324)	+0.18 (285)	+7.82 (232)	+[b]
	TFE			−1.93 (314)		+10.40 (238)	+22.4 (183)
	TFA/Oct			−1.57 (310)		+10.29 (242)	+[b]
7	Oct	114 (337)	6420 (233)	−1.72 (322)		−10.54 (230)	−[b]
	Ace	142 (333)	5900 (237)	−2.08 (321)		−11.10 (234)	−[b]
	Eth	167 (329)	5760 (239)	−1.79 (317)		−9.20 (236)	−[b]
	TFE	241 (321)	5320 (244)	−2.25 (310)		−9.68 (241)	−[b]
	TFA/Oct	239 (316)	5500 (246)	−2.26 (307)		−10.17 (244)	−[b]

[a] Oct = isooctane; Ace = acetonitrile; Eth = ethanol. TFE = 2,2,2-trifluoroethanol; TFA/Oct = 1% trifluoroacetic acid in isooctane. [b] Maximum not reached (−[b], +[b] positive, negative values, respectively).

Table 4. Low-Temperature CD Data of Enones **4** and **7** in Methylcyclohexane/Isopentane (1:3) [$\Delta\epsilon$ (λ_{max}/nm)]

	temperature, °C					
compd	+20	−20	−60	−100	−140	−160
4	−0.86 (332)	−0.96 (333)	−1.02 (333)	−1.08 (333)	−1.14 (332)	−1.14 (333)
	+0.23 (291)	+0.26 (291)	+0.28 (291)	+0.24 (291)	+0.20 (292)	+0.22 (291)
7	−2.42 (324)	−2.82 (324)	−3.03 (323)	−2.90 (325)	−2.82 (326)	
	+1.33 (257)	+1.06 (256)	+0.84 (257)	+1.12 (258)	+0.63 (264)	
	−13.02 (230)	−15.52 (231)	−14.73 (231)	−14.46 (230)	−15.34 (231)	

agrees with the *P* configurational type of enone **4** (Figure 4). According to our conclusion[2] the sign of this band is opposite to the sign of the nπ* CE.

Enone **7** (Table 3, Figure 5) exhibits in all solvents studied as well as in the whole temperature range (Table 4) a strong negative monosignate nπ* band in contradiction to the positive one expected on the basis of the positive enone torsion angle found by MMX calculation and X-ray analysis. Thus, it is the first case found by us when the sign of the cisoid enone torsion angle (positive) does not correlate with the sign of the nπ* CE (negative). The band I CE of enone **7** observed in the range of 230−240 nm is monosignate and strongly negative in all solvents studied (Table 3) although in a methylcyclohexane/isopentane mixture a relatively intensive positive CD maximum at about 260 nm additionally appears (Table 4). Its sign follows the original orbital enone helicity rule.[13] The sign of well-separated negative band II CE, which does not reach a maximum above 185 nm, agrees with the *M* configurational type of **7** (Figure 4). Similar to enone **4**, the enone **7** shows a blue shift of the nπ* CE and a red one of the band I CE on going from nonpolar to polar solvents (Table 3, Figure 5).

Circular Dichroism of Anisotropic Samples (ACD). The ACD (circular dichroism of oriented molecules[15−20]) and polarized UV spectra (absorption of parallelly and perpendicu-

(14) Gawronski, J. K. Conformations, chiroptical and related spectral properties of enones. In *The Chemistry of Enones*; Patai, S., Rappoport, Z., Eds.; John Wiley and Sons Ltd.: New York, 1989; pp 54−105.

(15) Kuball, H.-G.; Altschuh, J.; Schönhofer, A. *Chem. Phys.* **1979**, *43*, 67−80.

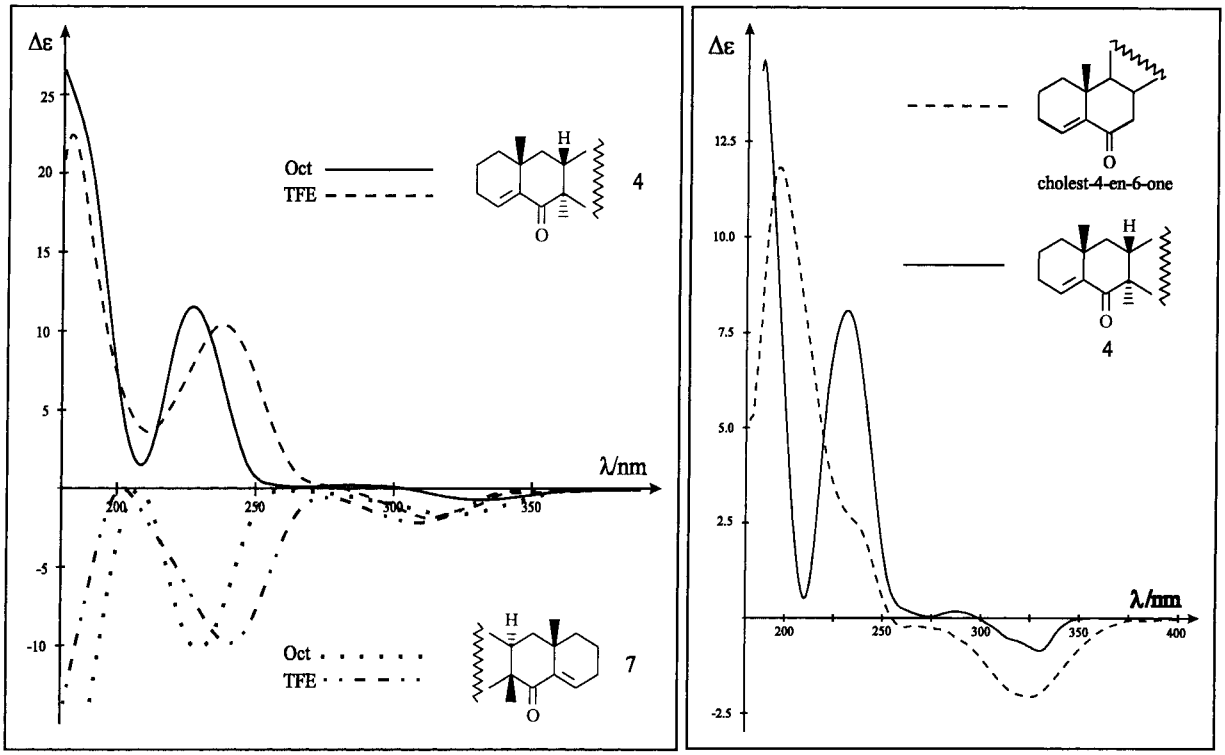

Figure 5. CD spectra of **4** and **7** in isooctane and trifluoroethanol (left) and of cholest-4-en-6-one and **4** in acetonitrile (right).

larly polarized light[21]) provide a refined structural information in addition to the UV and CD spectra. For the measurements of ACD and polarized UV molecules have to be brought into a partially ordered state (see Appendix and Experimental Section).

In ZLI-1695 (Merck) **4** and **7** show, as in the other solvents (Figure 5), a negative CD for the nπ* transition and a positive and a negative CD for the $\pi\pi$* transition and the band II CE, respectively. Against that the $\Delta\epsilon^{A}(T)$ curves within the nπ* transition are positive for **4** and negative for **7** whereas in both cases $\Delta\epsilon$ is negative (Figures 6 and 7, Tables 5 and 6). That is, $\Delta\epsilon^{A} - \Delta\epsilon$ is positive for **4** and negative for **7** (Figure 8) for all temperatures. Neglecting the contribution to the ACD determined by the small order parameter D* in eq A-1 (Appendix)—allowed within a good approximation—the signs of $\Delta\epsilon^{*}_{33}$ for the nπ* transition for **4** and for **7** are positive and negative, respectively. The latter statement together with eq A-3 imply with a high probability that $\Delta\epsilon^{*}_{11} + \Delta\epsilon^{*}_{22} < 0$ for **4** and $\Delta\epsilon^{*}_{11} + \Delta\epsilon^{*}_{22} > 0$ for **7**, at least from the measurements at low temperatures (Table 7). On the basis of these results (Table 7) one can conlude that the enone chromophores behave like local enantiomers. This is consistent with a negative [positive] torsional angle φ of the O(1)═C(1)—C(2)═C(1′) [C(1′)═C(2)—C(3)—C(28)] unit for **4** and a positive [negative] one for **7** derived from the X-ray data exhibiting approximately equal absolute values of enone torsional angle φ for **4** and **7**.

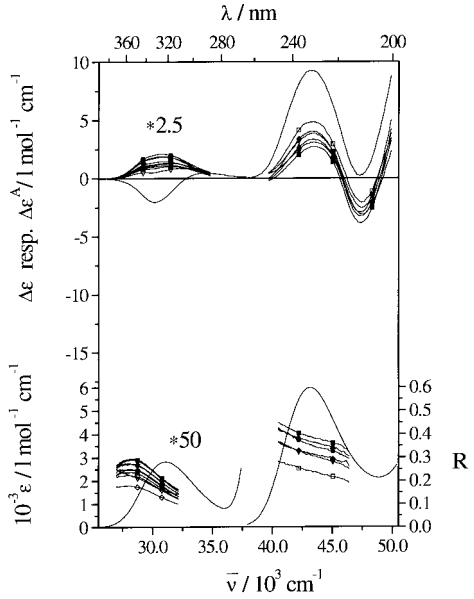

Figure 6. The CD spectra $\Delta\epsilon$ (—) and UV spectra ϵ (—) of **4** in ZLI-1695 (Merck) for $T = 75$ °C and the ACD spectra $\Delta\epsilon^{A}$ and the degree of anisotropy R for different temperatures. The symbols used for the identification of temperatures are given in Table 5.

If for the coordinates $\Delta\epsilon^{*}_{33}$ and $\Delta\epsilon^{*}_{11} + \Delta\epsilon^{*}_{22}$ a helicity rule can be used, the fact that **4** and **7** are local enantiomers would be correctly predicted, since for enantiomers or local enantiomers (under the experimental conditions used for the ACD measurements here), the coordinates change sign $\Delta\epsilon^{*}_{ii} \rightarrow -\Delta\epsilon^{*}_{ii}$ and thus $\Delta\epsilon \rightarrow -\Delta\epsilon$. Although the coordinates predict that **4** and **7** are local enantiomers, the sum of three independent contributions (eq A-3), i.e., the original helicity rule for $\Delta\epsilon$,

$$\Delta\epsilon = 1/3(\Delta\epsilon^{*}_{11} + \Delta\epsilon^{*}_{22} + \Delta\epsilon^{*}_{33}) \qquad \text{(A-3)}$$

predicts the wrong configuration for **7**. This contradiction can

(16) Kuball, H.-G.; Neubrech, S.; Schönhofer, A. *Chem. Phys*. **1992**, *163*, 115−132.
(17) Kuball, H.-G.; Schönhofer, A. *Polarized spectroscopy of ordered systems, optical activity of oriented molelcules*; Samori, B., Thulstrup, E. Eds.; NATO ASI Series C, Vol. 242; Kluwer: Dordrecht, 1988; pp 391−420.
(18) Kuball, H.-G.; Sieber, G.; Neubrech, S.; Schultheis, B. *Chem. Phys*. **1993**, *169*, 335- 350.
(19) Altschuh, J.; Karstens, T.; Kuball, H.-G. *J. Phys. E. Sci. Instrum.* **1981**, *14*, 43−44.
(20) Kuball, H.-G.; Schultheis, B.; Klasen, M.; Frelek, J.; Schönhofer, A. *Tetrahedron: Asymmetry* **1993**, *4*, 517−528.
(21) Michl, J.; Thulstrup, E. W. *Spectroscopy with Polarized Light:* VCH Publishers: New York, 1986.

Table 5. $\Delta\epsilon^A - \Delta\epsilon$ and R of **4** for Different Temperatures at 30 303 and 43 103 cm^{-1} in ZLI-1695 (Merck)[a]

$\Delta\epsilon^A(T) - \Delta\epsilon$(75 °C)/l mol^{-1} cm^{-1}				degree of anisotropy $R(T)$			
nπ^* region $\bar{\nu}$, cm^{-1}		$\pi\pi^*$ region $\bar{\nu}$, cm^{-1}		nπ^* region $\bar{\nu}$, cm^{-1}		$\pi\pi^*$ region $\bar{\nu}$, cm^{-1}	
T, °C	30 303	T, °C	43 103	T, °C	30 303	T, °C	43 103
37.0 (■)	1.55 ± 0.12	28.0 (■)	−6.63 ± 0.84	37.0 (■)	0.434 ± 0.007	28.0 (■)	0.390 ± 0.002
38.0 (●)	1.63 ± 0.12	38.0 (●)	−6.25 ± 0.36	38.0 (●)	0.425 ± 0.006	38.0 (●)	0.353 ± 0.004
48.0 (▲)	1.52 ± 0.12	48.0 (▲)	−5.97 ± 0.93	48.0 (▲)	0.396 ± 0.007	48.0 (▲)	0.368 ± 0.002
52.0 (▼)	1.37 ± 0.12	58.0 (▼)	−5.47 ± 0.31	52.0 (▼)	0.392 ± 0.013	58.0 (▼)	0.312 ± 0.001
56.0 (◆)	1.30 ± 0.12	63.0 (◆)	−5.27 ± 0.81	56.0 (◆)	0.365 ± 0.005	63.0 (◆)	0.317 ± 0.003
60.5 (□)	1.21 ± 0.12	67.5 (□)	−4.48 ± 0.18	60.5 (□)	0.357 ± 0.010	67.5 (□)	0.241 ± 0.010
62.0 (○)	1.26 ± 0.13			62.0 (○)	0.323 ± 0.007		
62.5 (△)	1.16 ± 0.12			62.5 (△)	0.339 ± 0.008		
66.5 (▽)	1.02 ± 0.12			67.5 (◇)	0.259 ± 0.005		
67.5 (◇)	1.01 ± 0.12						
$\Delta\epsilon$ ($\bar{\nu}_{max}$)	−0.81 ± 0.12 (30166)	$\Delta\epsilon$ ($\bar{\nu}_{max}$)	9.27 ± 0.15 (43103)	ϵ ($\bar{\nu}_{max}$)	56.5 ± 1.1 (31104)	ϵ ($\bar{\nu}_{max}$)	5976 ± 10 (43103)

[a] $\Delta\epsilon$ (75 °C) and ϵ (75 °C)/l mol^{-1} cm^{-1} at the maxima of the nπ^* and $\pi\pi^*$ bands.

Table 6. $\Delta\epsilon^A - \Delta\epsilon$ and R of **7** for Different Temperatures at 29 369 and 42 553 cm^{-1} in ZLI-1695 (Merck)[a]

$\Delta\epsilon^A(T) - \Delta\epsilon$(75 °C)/l mol^{-1} cm^{-1}				degree of anisotropy $R(T)$			
nπ^* region $\bar{\nu}$, cm^{-1}		$\pi\pi^*$ region $\bar{\nu}$, cm^{-1}		nπ^* region $\bar{\nu}$, cm^{-1}		$\pi\pi^*$ region $\bar{\nu}$, cm^{-1}	
T, °C	29 369	T, °C	42 553	T, °C	29 369	T,°C	42 553
33.0 (■)	−1.95 ± 0.07	28.0 (■)	15.5 ± 0.6	37.0 (■)	0.242 ± 0.002	28.0 (■)	0.002 ± 0.014
37.0 (●)	−1.84 ± 0.07	38.0 (●)	13.2 ± 1.6	38.0 (●)	0.257 ± 0.004	38.0 (●)	0.004 ± 0.001
48.0 (▲)	−1.64 ± 0.06	48.0 (▲)	13.7 ± 0.5	52.0 (▲)	0.211 ± 0.001	48.0 (▲)	0.003 ± 0.010
52.0 (▼)	−1.53 ± 0.06	58.0 (▼)	10.9 ± 1.3	58.0 (▼)	0.209 ± 0.002	58.0 (▼)	0.004 ± 0.002
58.0 (◆)	−1.37 ± 0.04	63.0 (◆)	10.7 ± 0.6	60.5 (◆)	0.189 ± 0.001	63.0 (◆)	0.003 ± 0.009
60.5 (□)	−1.27 ± 0.03	68.0 (□)	8.2 ± 0.6	67.5 (□)	0.162 ± 0.003	67.5 (□)	0.006 ± 0.003
62.5 (○)	−1.18 ± 0.03						
63.0 (△)	−1.16 ± 0.04						
65.0 (▽)	−1.04 ± 0.04						
$\Delta\epsilon$ ($\bar{\nu}_{max}$)	−1.72 ± 0.04 (30769)	$\Delta\epsilon$ ($\bar{\nu}_{max}$)	−8.3 ± 0.4 (42918)	ϵ ($\bar{\nu}_{max}$)	114.3 ± 0.7 (29630)	ϵ ($\bar{\nu}_{max}$)	6073 ± 59 (42283)

[a] $\Delta\epsilon$(75 °C) and ϵ(75 °C)/l mol^{-1} cm^{-1} at the maxima of the nπ^* and $\pi\pi^*$ bands.

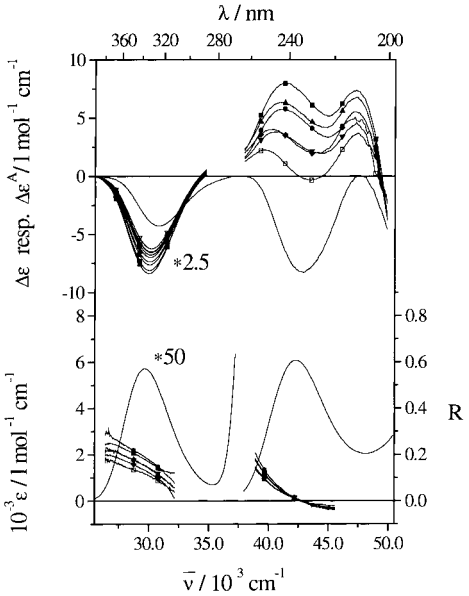

Figure 7. The CD spectra $\Delta\epsilon$ (—) and UV spectra ϵ (—) of **7** in ZLI-1695 (Merck) for T = 75 °C and the ACD spectra $\Delta\epsilon^A$ and the degree of anisotropy R for different temperatures. The symbols used for the identification of temperatures are given in Table 6.

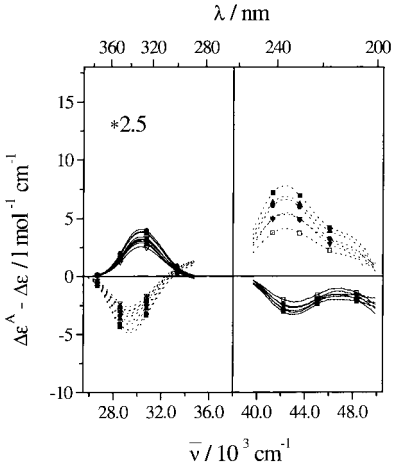

Figure 8. The different spectra $\Delta\epsilon^A - \Delta\epsilon$ of **4** (—) and **7** (···) in ZLI-1695 (Merck) for different temperatures. The symbols used for the identification of temperatures are given in Table 5 for **4** and in Table 6 for **7**.

Table 7. Sign of the Coordinates $\Delta\epsilon^*_{ii}$ of **4** and **7** for the nπ^* Transition

	$\Delta\epsilon^*_{33}$	$\Delta\epsilon^*_{11} + \Delta\epsilon^*_{22}$
4	>0	<0
7	<0	>0

be interpreted by a model proposed earlier:[18,22] The CD is the sum of three independent $\Delta\epsilon^*_{ii}$. Each coordinate $\Delta\epsilon^*_{ii}$ itself can be different in size and sign, in general. Furthermore, for local enantiomers $\Delta\epsilon^*_{11}$, $\Delta\epsilon^*_{22}$, and $\Delta\epsilon^*_{33}$ can vary in their size

(22) Kuball, H.-G.; Schönhofer, A. Circular Dichroism of Oriented Molecules. In *Circular Dichroism: Principles and Applications*; Nakanishi, K., Berova, N., Woody, R. W., Eds.; VCH Publishers: New York, 1994; pp 85−103.

(23) Nassimbeni, L. R.; Russell, J. C.; Cragg, G. M. L. *Acta Crystallogr.* **1977**, *B33*, 3755−3758.

(24) Lightner, D. A.; Flores, M. J.; Crist, B. V.; Gawronski, J. K. *J. Org. Chem.* **1980**, *45*, 3518−5522.

(25) Gawronski, J. K.; Liljefors, T.; Norden, B. *J. Am. Chem. Soc.* **1979**, *101*, 5515−5522.

differently as a consequence of different vibronic coupling induced by a variation of the surroundings of the chromophore, i.e., by forming different conformations with the same absolute configuration. Thus, by such a mechanism a sign change of $\Delta\epsilon$ can happen if the $\Delta\epsilon^*_{11}$, $\Delta\epsilon^*_{22}$, and $\Delta\epsilon^*_{33}$ are of different sign and vary within a series of compounds in their absolute values. Then, according to eq A-3 the summation over all coordinates $\Delta\epsilon^*_{ii}$ can result in a sign change for $\Delta\epsilon$ without a change of the absolute configuration.

Because $|\Delta\epsilon^A| > |\Delta\epsilon|$ on the long wavelength side of the nπ* band, we can assume that the allowed progression $\bar{\nu} = \bar{\nu}_{00} + n\bar{\nu}_1$ determines the coordinate $\Delta\epsilon^*_{33}$, whereas $\Delta\epsilon^*_{11} + \Delta\epsilon^*_{22}$ is mainly determined by a forbidden progression $\bar{\nu} = \bar{\nu}_{00} + \bar{\nu}_x + n\bar{\nu}_1$. Thus, it seems that the sign of $\Delta\epsilon$ is determined for **4** by the forbidden and for **7** by the allowed vibronic transitions of the nπ* band. Because the helicity rule is developed for the CD of the forbidden vibronic progression the rule must fail for **7**. The origin of this effect may result from the fact that in **4** and **7** the cyclohexene (A') and the cyclohexenone (A) rings have different conformations. Thus, the local enantiomeric chromophore "sees" different surroundings caused by the A' and A rings system (Figure 3). By the different perturbation from the surrounding the CD of the allowed progression decreases for **4** in comparison to **7** and the CD intensity of the forbidden progression increases (i.e., $|\Delta\epsilon^*_{33}|/|\Delta\epsilon^*_{11} + \Delta\epsilon^*_{22}|$ is >1 for **7** and < 1 for **4**) and thus, an apparently false CD signal for the nπ* transition is found for **7**.

With this interpretation the signs of the CD signal for the $\pi\pi$* transitions are in agreement for **4** and **7** with the enone helicity rule because in this case there is no vibronic coupling. That is, for the $\pi\pi$* transition the rules for the CD for local enantiomers are fulfilled.

Whether the severe solvent dependence of $\Delta\epsilon$ and ϵ found for isotropic solution (Table 3) is an effect of vibronic coupling cannot be proven. That is, this severe dependence cannot be understood and disscussed, at the moment.

This result demonstrates nicely a powerful application of the ACD spectroscopy for special problems. But one fact, which is approximately fulfilled for **4** and **7**, should be pointed out very clearly as discussed in the next section. The ACD spectra and thus the $\Delta\epsilon^*_{ii}$ of two compounds can only be compared directly if the orientations of the molecules or the chromophores under consideration in the molecule in the anisotropic phase are very similar. Otherwise the results obtained are not commensurable because of the special properties of the $\Delta\epsilon^*_{ij}$ tensor.

The Polarized Spectroscopy (Degree of Anisotropy). Whether there is a change of the orientation axis or the orientation of the chromophore with respect to the orientation axis can be analyzed with the polarized UV spectroscopy. In the liquid crystal host phase **4** and **7** are mainly oriented along the "orientation axis" which is an axis approximately along the longest molecular extension. With an often applied approximation the orientation axis is assumed to be approximately parallel to one of the principal axes of the tensor of inertia (the axis to which the smallest moment of inertia belongs). If the transition moment direction (the polarization direction) of the $\pi\pi$* transition of the >C═C−C═O chromophore is known with respect to the orientation axis then the order parameter *S** can be estimated (eq A-4, neglecting the D* term). From the orientation of the >C═C−C═O group, known from the X-ray structure, together with the results of the LD measurements of Nordén et al.,[25] in which the transition moment direction is given by the line connecting the C(1′)−carbon atom and the carbonyl oxygen, for **4** an *S** value of about 0.5 at 28 °C is obtained. A value of *S** (Appendix 2) of about 0.6−0.8 follows from the knowledge of the order of other ketosteroids[20] and from this a transition moment direction of about 33° against the orientation axis results. In contrast to **4** in **7** the A′ ring is oblique-angled against the main plane of the A, B, and C rings system. Thus, the orientation axis of **7** is more oblique to the transition moment direction than what is indicated by the fact that the degree of anisotropy of **7** is about zero (Figure 7) in contrast to $R \cong 0.3$ for **4** (Figure 6). An angle of about 54° is expected for **7** from the degree of anisotropy whereas for the line connecting the C(1′)−carbon atom and the carbonyl oxygen 68° results from the X-ray data. Thus, whereas the orientation axis in **4** is parallel to the C(1)−C(2) bond in the A ring, this axis has an angle of about 20° against the C(1)−C(2) bond direction in **7**. From *R* (**4**) > *R* (**7**) for the nπ* transition, this conclusion is supported. But for a rough estimation of the CD effects both axes with respect to the enone chromophore can be assumed to be approximately in the same direction.

From *R*($\pi\pi$* of **7**) < *R*(nπ* of **7**) < *R*(nπ* of **4**) < *R*($\pi\pi$* of **4**) follows that the nπ* transition is not uniformly polarized and thus the intensity stems essentially from vibronic contributions of different polarization. This conclusion is consistent with the general properties of nπ* transitions within cisoid and transoid enones. In addition to the result of the ACD measurement, it can be seen from R that the different band structures of the ACD and CD spectra of **4** and **7** (Figures 6 and 7) show also that different vibrations contribute to the ACD and CD spectra in different spectral regions.

Discussion

The perspective views of the structure of **4** and **7** in the crystalline state show the different conformations (Figure 2), particularly visible in the A and A′ rings, caused by the change of the methyl group configuration at C-3 from 3α for enone **4** (*trans-cisoid*-5,3 condensation in the vicinity of the chromophore) to 3β for enone **7** (*trans-transoid*-5,3 condensation). These structural differences can also be seen from the comparison of the torsion angle values given in Table 2. Ring A of compound **4** adopts a fairly symmetrical chair conformation and its perspective view along O→C carbonyl double bond is shown in Figure 3a (C, chair). Ring A′ is quasi trans condensed to ring A and has distorted HC (3′β, 4′α) conformation, as demonstrated in Figure 3b. Ring A of compound **7** exists in a slightly distorted boat conformation and its perspective view along the O→C carbonyl double bond resembles that shown in Figure 3a (NB − nonsymmetrical boat). Similarly as in the case of **4**, ring A′ of **7** is quasi trans condensed to ring A and adopts a slightly distorted HC (3′α, 4′β) conformation (Figure 3b, inverted HC, half chair). It is noteworthy at this stage that the geometries for the gaseous state of enones **4** and **7** calculated by the MMX program, described before, are in good agreement with these obtained from X-ray analysis. The calculated values of the torsion angles O(1)═C(1)−C(2)═C(1′) of the enones **4** and **7** are −56° and +52°, respectively, whereas the values experimentally found by X-ray analysis are equal to −45.9° for **4** and +56.5 for **7**. This gives a good hint that these conformers are also present in the solution.

The CD data of enone **4** can be compared with those of cholest-4-en-6-one[1] (Figure 5, right), which represents the enone of the same *P* configurational type and possesses similar geometric parameters.[24] The comparison of both these compounds shows that the axial methyl group at C-10 (α′-axial alkyl substituent) seems to be responsible for the appearance of the

weak positive part of the nπ* CE in **4** and the low intensity of the negative part of this effect. Compared with cholest-4-en-6-one, enone **4** exhibits an absence of the weak negative part of band I CE and about a 3 times stronger positive part of this CE. The blue shift of the band II CE of enone **4**, as well as of enone **7**, with regard to α'-unsubstituted cholest-4-en-6-one (shown in Figure 5) may be attributed to the presence of two σ C−C bonds at the α'-position.

The change of the configuration of the methyl group at C-3 from 3α for enone **4** to 3β for enone **7** (Scheme 1) changes the helicity of C(1′)═C(2)−C(3)−C(28) as well as the enone helicity and makes the surroundings of the cyclohexene units of **4** and **7** quasi-enantiomeric. Therefore, the CD curves of **4** and **7** are quasi mirror images below 270 nm (Figure 5, left). The major difference between those two enones, being the result of the above-mentioned configurational change of the methyl group, is the conformation of the cyclohexanone unit—slightly distorted symmetrical chair for **4** and nonsymmetrical boat for **7**. The nonsymmetrical boat conformation of cyclohexanone unit of **7** may be the reason of its abnormal chiroptical behavior within the nπ* absorption range. The ACD spectra provide an interpretation for the negative CD of **4** and the negative CD of **7** in this region, namely that the CD of **4** and **7** results from different vibronic progressions. This means that the vibronic coupling originated by the different surroundings of the enone chromophore of **7** intensifies the CD coordinates of eq A-3 in such a way that the positive contribution of $\Delta\epsilon^*_{11} + \Delta\epsilon^*_{22}$ is overcompensated by the negative contribution of $\Delta\epsilon^*_{33}$. Here the helicity rule should be applied to $\Delta\epsilon^*_{11} + \Delta\epsilon^*_{22}$ instead of $\Delta\epsilon$ because helicity rules can only be applied to the CD of the same transitions. If this is true, the negative sign of the nπ* CE of **7** stems from the vibronic coupling induced by the cyclohexanone ring, causing an intensification of the allowed progression relative to the forbidden progression. In general, for an achiral cyclohexanone moiety as found for **4**, the CD of the forbidden vibronic progression determines the CD of the isotropic solution, which is the case for which the helicity rule has been developed.

There is a second sign change which can be discussed in the same way. Although in the α'-position of **7** two σ C−C bonds are present, their contributions cancel each other, owing to their bisecting conformation. Thus, enone **7** shows a monosignate nπ* CE without an additional positive part at shorter wavelength, as in the case of enone **4**.

Conclusions

(i) If a cyclohexanone unit of a cisoid enone adopts a symmetrical or slightly distorted symmetrical chair or boat conformation (achiral cyclohexanone ring) the sign of the monosignate band or the sign of the long wavelength part of bisignate band within the nπ* absorption transition is governed by the enone helicity rule, i.e., it corresponds to the sign of the enone torsion angle.

(ii) If a cyclohexanone unit adopts a non-symmetrical conformation, the sign of the nπ* CE correlates with the chirality of the cyclohexanone ring, and the double bond probably behaves as a common α-substituent. This case resembles that of planar cisoid enones whose sign of the nπ* CE is correspondingly the same as the nπ* CE of parent ketones without the exomethylene (exoalkylidene) group.[14,25]

(iii) The rule connecting the sign of the Band II CE with enone stereochemistry is now slightly modified, i.e., the sign of this CE is governed by helicity of the C(1′)═C(2)−C(3)−C(28) (*P* or *M*) and is here opposite to the sign of the enone torsion angle (enone helicity).

(iv) From the results of the ACD measurements it follows that the apparent break down of the helicity rule for the nπ* transition of cisoid enone chromophore of **7** is a consequence of an intensification of the contribution of the allowed vibronic progression to the CD. Thus, the allowed progression determines the negative CD of the isotropic solution for the cisoid enone **7** with the *P* enone helicity. In contrast to that, the negative CD for **4** with the *M* enone helicity is determined by the forbidden progression (Figure 4). This confirms the conclusion that sector or helicity rules can only be applied to a CD which belongs to the same type of vibronic transition for which the rule was developed.

Experimental Section

To measure circular dichroism for anisotropic samples (ACD),[15−17,22] compensated nematic or nematic liquid crystal phases (guest/host system) are suitable to align partially the chiral compounds **4** and **7**. The chiral guest transforms the nematic phase to a cholesteric phase (chiral induction) which by itself exhibits a large CD and ORD as a property of the phase. This CD and ORD originated by the phase is orders of magnitudes larger than the CD and ORD of the molecules and, therefore, for the ACD measurement the sample has to be transformed in a nematic phase again. This can be done for compensated cholesteric phases by adjusting the temperature to the nematic temperature T_N of the guest/host system and applying an electric ac or dc field (10^6 V/m). For the induced cholesteric phase, originating from a nematic phase, the nematic phase can be obtained by applying an electric ac or dc field large enough to unwind the helix (10^6 V/m). By this electric field the phase is transformed to a uniaxial liquid crystal unidomain with its optical axis (symmetry axis) parallel to the electric field.

The sample, filled in a special cuvette,[19] and then adjusted in a commercial CD instrument with the optical axis parallel to the propagation direction of the light beam enables the measurement of the ACD. The sample is free of linear dichroism effects if the measured effect is independent of rotation of the sample (cuvette) about the propagation direction of the light beam. The experimental procedure starts at first with a measurement of the isotropic solution at $T = 75$ °C ($\Delta\epsilon$), then the ACD measurements ($\Delta\epsilon^A$) ensue, and finally $\Delta\epsilon$ is measured again to check the stability of the sample. The error of $\Delta\epsilon$ is about 2% whereas that of $\Delta\epsilon^A$ is around 5 to 20%. For the liquid crystal phase host phase, ZLI-1695 (Merck mixture of four 4*n*-alkyl-4′-cyanobicyclohexanes) has been used throughout this paper for orienting the guest molecules.

Melting points were determined on a Boetius micromelting point apparatus and are uncorrected. IR spectra were recorded on a Perkin-Elmer PE 1310 spectrometer in CCl_4 solution. ^{1}H NMR spectra were taken on a Bruker AM-400 spectrometer in $CDCl_3$. Mass spectra were measured on a Varian MAT CH-5 and a VG AutoSpec (high resolution) spectrometer. UV measurements were made on a Philips PU 8740 or on a Cary 1E spectrophotometer in acetonitrile. CD spectra were recorded with a modified ISA-Jobin-Yvon Dichrograph Mark III or Aviv 62 DS. Solutions with concentrations in the range 0.2−0.5 mg/mL were examined in the cells with path length 0.05−2 cm. Column chromatography was performed on Kieselgel (Merck) 60 (63−200 μm).

3-(3-(5,5-Dimethyl-1,3-dioxane-2-yl)-propyl)-5α-cholest-2-en-1-one (2). Magnesium turnings (1 g) were placed into an argon-filled flask and covered with 5 mL of dry THF. 2-(3-Bromopropyl)-5,5-dimethyl-1,3-dioxane (7 g, Riedel de Häen) was then added over 5 min at room temperature. Smooth heating was necessary to start the Grignard reaction. After the mixture was stirred for 30 min 5α-cholest-1-en-3-one (4 g)[26] was added. The reaction mixture was stirred for 2 h and then diluted with saturated ammonium chloride solution (20 mL) slowly at 0 °C. After stirring overnight the mixture was extracted with ether and the combined organic layers were washed with water, dried,

(26) Green, G. F. H.; Long, A. G. *J. Chem. Soc.* **1961**, 2532−2543.

and evaporated. The crude product [3-(3-(5,5-dimethyl-1,3-dioxane-2-yl)propyl)-5α-cholest-1-en-3-ol] was dissolved in dry methylene chloride (100 mL), pyridinium dichromate (5 g) was added, and the mixture was stirred overnight. After dilution with 100 mL of ether, it was passed through a small silica gel column. The crude product was purified by column chromatography. Yield: 2.2 g (39%). Mp: 87 °C (ethanol), IR: 2960, 2870, 2850, 1720, 1675, 1640 cm^{-1}. ^1H NMR (400 MHz): 0.65 (3H, s, 18-H), 0.69 (3H, s, 5-Me dioxane), 0.98 (3H, s, 19-H), 1.16 (3H, s, 5-Me dioxane), 3.39 and 3.57 (4H, d, $J = 10.9$ Hz, 4- and 6-H dioxane), 4.40 (1H, t, $J = 4.6$ Hz, 2-H dioxane), 5.62 (1H, s, 2-H). MS: 540 (M^+), 525, 497, 436, 141 (100%). HRMS for $C_{36}H_{60}O_3$ (M^+): found 540.4549, calcd 540.4542.

3β-(3-(5,5-Dimethyl-1,3-dioxane-2-yl)propyl)-3α-methyl-5α-cholestan-1-one (3). Copper(I) iodide (0.95 g) was placed into a flask and covered with 12 mL of dry THF. The solution was cooled to −78 °C and 6.3 mL of methyllithium (1.6 M solution in ether) was added. The mixture was allowed to warm until all copper(I) iodide was dissolved. Then it was again cooled to −78 °C and BF_3-Et_2O (1.2 mL) was added. A solution of enone **2** (2.10 g) in THF (8 mL) was added dropwise, and the reaction mixture was stirred for 2 h at −78 °C. It was worked up as in case of compound **2** and purified by column chromatography. Yield: 1.75 g (81%). Mp: 131−133 °C (ethanol). IR: 2960, 2880, 2860, 1710, 1230 cm^{-1}. ^1H NMR: (400 MHz): 0.61 (3H, s, 18-H), 0.69 (3H, s, 5-Me dioxane), 0.84 (3H, s, 3-Me), 1.06 (3H, s, 19-H), 1.16 (3H, s, 5-Me dioxane), 1.73 (1H, dd, $J = 11.8$ and 1.6 Hz, 2a−H), 2.60 (1H, d, $J = 11.8$ Hz, 2b−H), 3.39 and 3.57 (4H, d, $J = 11.2$ Hz, 4- and 6-H dioxane), 4.38 (1H, t, $J = 4.9$ Hz, 2-H dioxane). MS: 556 (M^+), 541, 513, 399, 115 (100%). HRMS for $C_{37}H_{64}O_3$ (M^+): found 556.4855, calcd 556.4855.

3-Methyl-3α,5α-3,3′,4′,5′-tetrahydrobenzo[2,3]cholest-2-en-1-one (4). A solution of ketone **3** (1.0 g) in THF (150 mL) and concentrated HCl (60 mL) was refluxed for 2 days. It was then extracted with ether, and the organic layer was washed with water, sodium bicarbonate solution, and brine. After the mixture was dried and the solvent evaporated, the crude product was purified by column chromatography. Yield: 0.38 g (47%). Mp 165 °C (ethanol). IR: 2940, 2880, 1680, 1640 cm^{-1}. ^1H NMR (400 MHz): 0.63 (3H, s, 18-H), 0.95 (3H, s, 3-Me), 1.00 (3H, s, 19-H), 2.07 (2H, m, 5′−H), 5.78 (1H, t, $J = 3.7$ Hz, 6′−H). MS: 452 (M^+), 437, 424, 409, 329, 297, 43 (100%). HRMS for $C_{32}H_{52}O$ (M^+) found 452.4001, calcd 452.4018.

3-Methyl-5α-cholest-2-en-1-one (5).[27] 5α-Cholest-1-en-3-one (7.0 g) was dissolved in 80 mL of dry ether, and 12.6 mL of methyllithium (1.6 M in ether) was added at 0 °C. After stirring for 40 min, the solution was dilluted with 10% ammonium chloride solution (50 mL). The organic layer was separated and washed with water and brine. The crude product (3-methyl-5a-cholest-1-en-3-ol) was dissolved in methylene chloride and pyridinium dichromate (16 g) was added. The reaction mixture was stirred at room temperature for 25 h, evaporated to a volume of 60 mL, diluted with ether (150 mL), and filtered through a small silica gel column. The crude product was purified by column chromatography. Yield: 3.5 g (48%). Mp: 108 °C (methanol). IR: 1675, 1650 cm^{-1}. ^1H NMR (400 MHz): 0.65 (3H, s, 18-H), 0.99 (3H, s, 19-H), 1.83 (3H, s, 3-Me), 1.98 (1H, dd, $J = 18.9$ and 4.8 Hz, 4α-H), 2.12 (1H, m, 4β-H), 2.40 (1H, m), 5.61 (1H, s, 2-H). MS: 398 (M^+), 383, 355, 136 (100%).

3α-(3-(5,5-Dimethyl-1,3-dioxane-2-yl)-propyl)-3β-methyl-5a-cholestan-1-one (6). Magnesium turnings (0.75 g) were placed into a nitrogen-filled flask and covered with 5 mL of dry THF. 2-(3-Bromopropyl)-5,5-dimethyl-1,3-dioxane (5.7 g) was added slowly while the mixture was smoothly warmed until the Grignard reaction started. After the mixture was cooled to −78 °C, a solution of $CuBr[Me_2S]$ (0.5 g)[28] in Me_2S (3 mL) was added. Enone **5** (3.2 g) was dissolved in THF (8 mL) and added dropwise to the reaction mixture. The mixture was stirred for 3 h at −78 °C and worked up as in case of **2**. Yield: 2.9 g (65%). Mp: 94 °C (ethanol). IR: 2950, 2870, 1705, 1470, 1230 cm^{-1}. ^1H NMR (400 MHz): 0.61 (3H, s, 18-H), 0.69 (3H, s, 5-Me dioxane), 0.94 (3H, s, 3-Me), 1.08 (3H, s, 19-H), 1.15 (3H, s, 5-Me dioxane), 1.85 (1H, dd, $J = 12.1$ and 1.9 Hz, 2α-H), 2.54 (1H, d, $J = 12.2$ Hz, 2β-H), 3.38 (2H, dd, $J = 11.0$ and 2.0 Hz, 4- and 6-H dioxane), 3.56 (2H, td, $J = 11.0$ and 2.1 Hz, 4- and 6-H dioxane), 4.37 (1H, t, $J = 5.0$ Hz, 2-H dioxane). MS: 556 (M^+), 469, 399, 115 (100%); HRMS for $C_{37}H_{64}O_3$ (M^+): found 556.4852, calcd 556.4855.

3-Methyl-3β,5α-3,3′,4′,5′-tetrahydrobenzo[2,3]cholest-2-en-1-one (7). A solution of ketone **6** (2 g) in 160 mL of dioxane and 100 mL of concentrated HCl was refluxed for 24 h and worked up as in case of **4**. Separation of the two main products was done by column chromatography (hexane/toluene 2:1). The first eluate was identified as the unconjugated enone **8**, and the second was the desired enone. Yield: 0.74 g (45%). Mp 109 °C (ethanol). IR: 2940, 2870, 1685, 1635, 1470 cm^{-1}. ^1H NMR (400 MHz): 0.64 (3H, s, 18-H), 1.00 (3H, s, 19-H), 1.02 (3H, s, 3-Me), 1.68 (2H, m, 4′−H), 2.12 (2H, m, 5′−H), 5.93 (1H, t, $J = 3.6$ Hz, 6′−H). ^{13}C NMR (100 MHz): 212.4 (1-C), 147.8 (2-C), 130.1 (6′-C), 56.8, 56.6, 50.1, 50.0, 42.7, 42.2, 41.9, 40.2, 39.7, 37.4, 36.4, 36.0, 35.8, 33.1, 31.9, 29.5, 28.4, 28.2, 27.9, 25.1, 24.6, 24.1, 23.13, 23.06, 22.8, 18.8, 18.7, 12.4, 11.6; MS: 452 (M^+), 437, 424, 193, 175 (100%). HRMS for $C_{32}H_{52}O$ (M^+): found 452.4013, calcd 452.4018.

3-Methyl-2β,3β,5α-2,3,3′,4′-tetrahydrobenzo[2,3]cholest-2-en-1-one (8). Yield: 0.46 g (28%). Mp: 174 °C (ethanol); IR: 3040, 1705 cm^{-1}; ^1H NMR (400 MHz): 0.62 (3H, s, 18-H), 1.05 (3H, s, 19-H), 1.14 (3H, s, 3-Me), 3.05 (1H, d, $J = 5.2$ Hz, 2β-H), 5.46 (1H, m, 6′−H), 5.81 (td, $J = 10.0$ and 3.4 Hz, 5′−H). MS: 452 (M^+), 424, 330, 94 (100%). HRMS for $C_{32}H_{52}O$ (M^+): found 452.4011, calcd 452.4018.

Acknowledgment. This work was partially supported by Polish Academy of Sciences and Deutsche Forschungsgemeinschaft also with the Grant No 436 POL 113-38. Financial support from the "Fonds der Chemischen Industrie" is gratefully acknowledged.

Appendix. Working Equations for ACD

For an ensemble of partially oriented molecules with a uniaxial orientational distribution and a light beam propagating parallel to the optical axis of the sample, the ACD ($\Delta\epsilon^A$) is connected with the molecular quantities $\Delta\epsilon^*_{ii}$ by

$$\Delta\epsilon^A - \Delta\epsilon = (\Delta\epsilon^*_{33} - \Delta\epsilon)S^* + {}^1/_3(\Delta\epsilon^*_{22} - \Delta\epsilon^*_{11})D^* \quad \text{(A-1)}$$

$\Delta\epsilon$ is the CD of the isotropic solution. S^* and D^* are the Saupe order parameters given with respect to the principal axes x^*_i of the order tensor and the molecular quantities $\Delta\epsilon_{ij}$ ($i,j = 1-3$), the coordinates of the circular dichroism tensor, are also given with respect to x^*_i coordinate system.[17] $\Delta\epsilon^*_{ii}$ can be understood as a result of measurement with oriented molecules with a special orientation distribution. For example, for the uniaxial sample with $S^* = 1$ and $D^* = 0$ all molecules are oriented parallel with their orientation axis x^*_3, whereas the x^*_1 and x^*_2 axes are equally distributed about this direction. S^* and D^* can be determined by polarized spectroscopy in the IR or UV spectral region or with NMR spectroscopy. S^* describes the orientational order with regard to one axis, the orientation axis (x^*_3), within the molecule. For the qualitative discussion the direction parallel to the longest extension of the molecule can be chosen as the orientation axis. In the exact description this is the principal axis of the order tensor to which the largest eigenvalue belongs. The order parameter D^* is, roughly speaking, a quantity which is a measure of the deviation from a rotational symmetry of the orientational distribution about the orientation axis (for an exact description of these axes see refs 15−17 and 22).

For a light beam propagating parallel to this axis from eq A-1 follows

(27) Cocton, B.; Crustes de Paulet, A. *Bull. Soc. Chim. Fr.* **1966**, 2947−55.

(28) House, H. O.; Chu, C. Y.; Wilkins, J. M.; Umen, M. J. *J. Org. Chem.* **1975**, *40*, 1460−1469.

$$\Delta\epsilon^{A} = \Delta\epsilon^{*}_{33}$$

That means, $\Delta\epsilon^{*}_{33}$ is the result of a CD measurement with a light beam propagating along the x^{*}_{3} direction. For $\Delta\epsilon^{*}_{11}$ and $\Delta\epsilon^{*}_{22}$ it is not possible to give such a simple recipe for direct measurement. But these values can be understood in the same way as a result of measurements with light beams propagating either along the x^{*}_{1} or the x^{*}_{2} direction, but for the corresponding measurement the molecules have to be distributed rotationally symmetric about the or the axis.

The CD of the isotropic solution $\Delta\epsilon$ can be given here by

$$\Delta\epsilon = {}^{1}/_{3}(\Delta\epsilon^{*}_{11} + \Delta\epsilon^{*}_{22} + \Delta\epsilon^{*}_{33}) \qquad \text{(A-3)}$$

In an ideal, but for liquid crystals not realizable, case, $\Delta\epsilon$ has to be measured at the same temperature as $\Delta\epsilon^{A}$. With the measured value $\Delta\epsilon$ for the isotropic solution $\Delta\epsilon^{*}_{11}$, $\Delta\epsilon^{*}_{22}$, and $\Delta\epsilon^{*}_{33}$ can be obtained using additionally eq A-3.[20]

Analogous to eq A-1 the degree of anisotropy R for the polarized UV absorption can be described by the order of the system

$$R = \frac{\epsilon_1 - \epsilon_2}{\epsilon_1 + 2\epsilon_2} \qquad \text{(A-4)}$$

$$3\epsilon R = {}^{1}/_{2}(\epsilon^{*}_{33} - \epsilon)S^{*} + \sqrt{\frac{3}{2}}(\epsilon^{*}_{33} - \epsilon^{*}_{11})D^{*}$$

with $3\epsilon = \epsilon_{11} + \epsilon_{22} + \epsilon_{33} = \epsilon_1 + 2\epsilon_2$. Here, ϵ_1 and ϵ_2 are the absorption coefficient for light polarized parallel and perpendicular to the optical axis of the uniaxial sample, respectively.

Supporting Information Available: Crystallographic details for compounds **4** and **7** (including atomic coordinates, anisotropic displacement parameters, bond lengths, bond angles and torsion angles), in CIF format, are available through the Internet only. See any current masthead pages for access instructions.

JA973076C